Journal of Sensor Science and Technology
Vol. 22, No. 3 (2013) pp. 185-190
http://dx.doi.org/10.5369/JSST.2013.22.3.185
pISSN 1225-5475/eISSN 2093-7563

Morphology of CD4+ T Lymphocytes Bound on Nano-Patterened Substrates for Sensing the Size of Nanoholes

Dong-Joo Kim[1], Gil-Sung Kim[1], Yong-Deuck Woo[2], and Sang-Kwon Lee[3,+]

Abstract

We report on direct finding of how the morphology (i.e. filopodia width) of CD4+ T lymphocytes correlates with the size of the quartz nanohohole arrays (QNHAs, 140, 200, 270, and 550 nm in diameter) via scanning electron microscopy (SEM). This research exhibits that the filopodia of CD4+ T-lymphocytes extended on the QNHA substrates were observed to increase in width by increasing the size of QNHA in diameter from 140 to 550 nm. This strong linear response (R^2=0.988, n = 6) in filopodia's width of surface-bound CD4+ T-cells with topographical structures of QNHA can be explained by contact guidance between the cells and solid-state substrates. Furthermore, this research suggests that the protruded filopodia of surface-bound T-lymphocytes can be used as a biosensor for sensing the topographical information of the nano-patterned substrates.

Keywords : Quartz nanohole arrays, Biomedical sensors, Contact guidance, Filopodia, Microvilli, T-lymphocytes

1. INTRODUCTION

In last decades, the application of nanotechnology in the fields of electronic and optical engineering was well established [1-3]. Furthermore, nanostructures have been increasingly used for studies on cell interaction with solid nanostructures because unique properties of nanostructured surfaces enable a variety of novel functions of immobilized cells on the nanostructured surfaces [4, 5]. To date, these nanostructures were prepared by various methods including the polymeric templating method [6], vapor-liquid-solid (VLS) growth [7], dry-etching process using nanosphere lithography technique [8, 9]. Recently, we have also demonstrated a novel platform for separating CD4+ T lymphocytes from mouse splenocytes using streptavidin (STR)-functionalized and vapor-liquid-solid (VLS)-grown silicon nanowire (SiNW) [7] as well as transparent quartz nanopillar (QNP) arrays [8, 9] having a higher separation efficiency of 93-95.3%. However, there is no study on how the various size and shape-matched nanostructures and nanomaterials interact in the primary cells on the nanostructured substrates. Herein, we bring to direct investigation of how filopodia, which are tiny hairlike folds in the plasma membrane that extend from the surface of many T-lymphocytes, morphologies (e.g. width etc.) of T-lymphocytes, react to the different size of quartz nanohole arrays (QNHAs). In addition, we investigate the how regular nanohole structures (ranging of 140 to 550 nm) influence the formation of the filopodia of CD4+ T-lymphocytes bound on the QNHA substrates. On the basis of our results, the morphology of surface-bound CD4+ T-cells was highly related to the size of the QNHA structures. In addition, we found that the primary live T-cells could be a good biosensor to detect the size of the underneath nanostructures.

According to recent studies, cell adhesion is significantly affected by surface chemical composition and nanotopography, providing the cell adhesion can be increased or decreased depending on the materials and geometry of the substrate underneath the cell [10]. Based on previous researches, we have found the proper condition of QNHA by analysis of the cell adhesion morphologies on various QNHA, then confirmed that it is available to develop the sensor of disease diagnosis (i.e. AIDS [11], cancer [12], Alzheimer's disease [13] etc.)

[1]Department of Semiconductor Science and Technology, Chonbuk National University, Jeonju 561-756, Korea
[2]Department of Mechanical and Automotive Engineering, Woosuk University, Wanjugun 565-701, Korea.
[3]Department of Physics, Chung-Ang University, Seoul 156-756, Korea
[+]Corresponding author: sangkwonlee@cau.ac.kr
(Received : Apr. 4, 2013, Revised : May. 6, 2013, Accepted : May. 17, 2013)

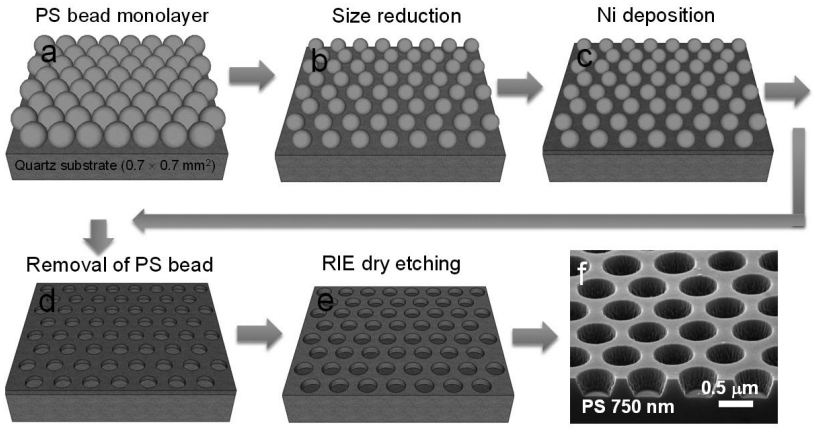

Fig. 1. (a-e) Schematic diagrams outlining the fabrication of quartz nanohole arrays (QNHAs). (f) SEM image of as-prepared QNHAs using 750-nm polystyrene nanoparticles.

using optimal QNHA substrate by detection of target cell with high yield and purity. Especially, the diagnosis of cancer using circulating tumor cells (CTCs) detection by nanostructure has been reported predominantly promising technologies including immunomagnetic bead and cell size based separation and microfluidics technology for capturing the targeted CTCs [14].

2. EXPERIMENTAL

2.1 Quartz nanohole array (QNHA) fabrication

Figs. 1a-f show the schematic view of the several QNHA fabrication processes including polystyrene (PS) monolayer deposition (Fig.1a), PS size reduction (Fig. 1b), Ni metal deposition as an etching mask (Fig. 1c), PS bead removal (Fig. 1d), and reactive ion etching of quartz substrates (Fig. 1e). The detailed processes are as follows. To fabricate the QNHA structures on quartz substrates, colloidal PS suspension containing different sizes of PS nanoparticles NPs) (200, 300, 430, and 750 nm in diameter) was first carefully deposited on the QNHA substrate using a modified self-assembly technique we improved previously (Fig. 1a) [9]. To create space between the spin-coated PS NPs, their sizes were first reduced by O_2 plasma etching for 5 s (O_2/Ar=35/10 sccm, RF power of 100 W and bias power of 50 W). 25-nm Ni metallization onto the coated surface of PS NPs was performed (Fig. 1c) and the PS NPs were subsequently removed by ultrasocication in N-methyl-2-pyrrolidone (Fig. 1d). Second RIE process was then performed for 40 s (CF4/Ar=40/5 sccm, RF power of 100W, and bias power of 50 W) to create the QNHA on the substrates (Fig. 1e). Finally, the remnant of Ni metal layer was completely removed using wet-chemical etching process (Fig. 1f).

2.2 QNHA surface functionalization

QNHA substrates (7 mm × 7 mm) were carefully cleaned with H_2O_2 : H_2SO_4 (1:1) for 10 min to remove all of the organic materials and impurities on the surface. We then washed the substrates using a three-step cleaning process (acetone, isopropyl alcohol, and distilled water) and dried them with air. The QNHA surface was first treated with O_2 plasma for 20 s to confer the hydroxyl groups on the QNHA surface after piranha cleaning process (96%H_2SO_4:30%H_2O_2=1:1) for 10 min. Next, the surface was applied by a three-step surface functionalization process using 1% (v/v) (3-aminopropyl)-triethoxysilane (APTES) in ethanol for 30 min at room temperature, 12.5% (v/v) glutaraldehyde (GA) in distilled water for 4 hr on a 3D-rocker, and 50 μg/mL streptavidin (STR) solution in phosphate buffered saline (PBS) overnight in an incubator (37°C, 5% CO_2). The QNHA samples are ready to collect incoming cell suspension containing primary mouse CD4 and CD8 T-lymphocytes, natural killer (NK), natural killer T (NKT), and B cells. We used this surface functionalized method to separate targeting specific cells (in our case $CD4^+$ T-lymphocytes) among different kinds of cells via novel STR-biotin conjugation technique to capture the incoming targeting cells in PBS solution as we reported previously [8, 9]. More detailed information can be found in previous reports [8, 9].

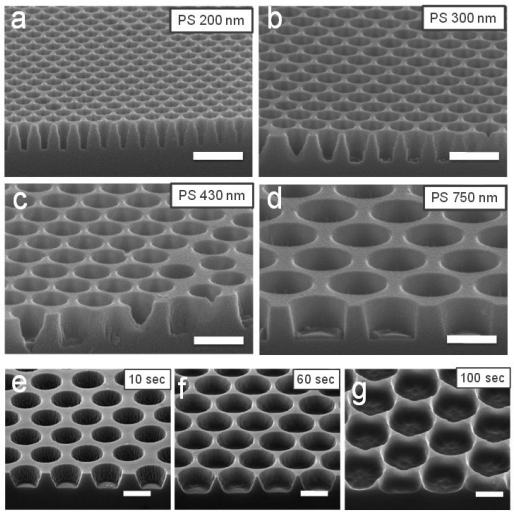

Fig. 2. (a-d) SEM images of QNHAs with different diameters (140, 200, 270, and 550 nm) prepared with four different sizes of PS nanoparticles (200, 300, 430, and 750 nm in diameter). (e-g) SEM images of the QNHAs with different period of BOE etching (10, 60, and 100 sec). For this experiment, 550-nm QNHAs were used. Scale bar is 0.5 ㎛.

2.3 Cell preparation

In this study, T-lymphocytes were selected because they are an important immunocyte in the human body and have fundamental functions in the immune response to various diseases. These splenocytes were prepared from the spleens of C57BL/6/mice as described previously [7]. Prior to loading the cell suspension containing certain quantity of cells (~10^5 cells/mL) in the culture medium onto the QNHA substrates, the cell population with a final volume of ~30 ㎕was first reacted with biotinylated anti-CD4 mAb and incubated at 4°C for 20 min. Following incubation for 20 min, which is at the very early stage of cell adhesion on the substrates, with STR-conjugated QNHA substrates at 4 °C, unbound cells were removed by rinsing with phosphate buffered saline (PBS), while separated $CD4^+$ T cells could bind to STR-QNHA surfaces due to adhesion enabled by strong STR-biotin interaction. This process was repeated at least three times for 10 min on a 2-D rocker to completely remove non-specifically unbound cells from the QNHA substrate.

2.4 Morphology observation of surface-bound cells on QNHA substrate

To verify the morphologies of the captured $CD4^+$T lymphocytes bound on STR-conjugated QNHA substrates, a field effect scanning electron microscope (FE-SEM)

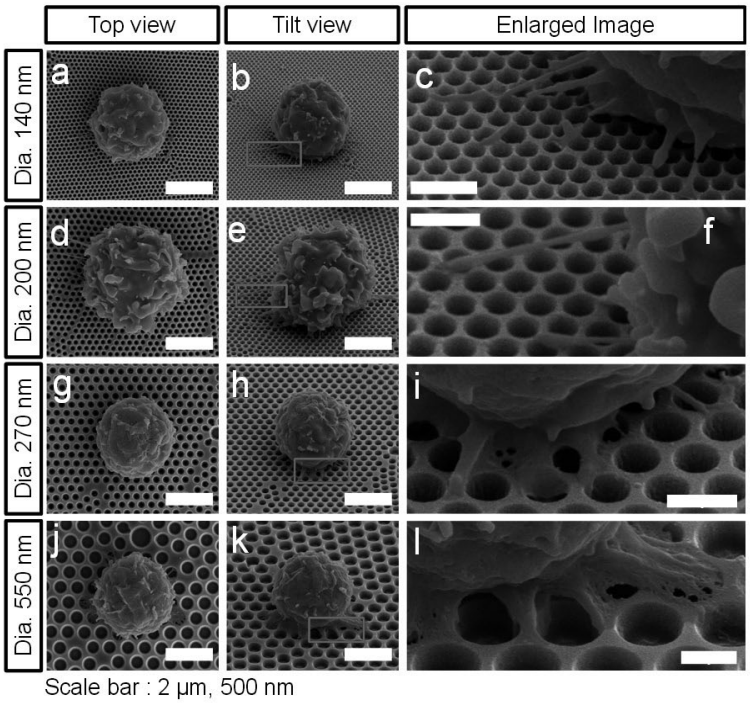

Fig. 3. (a-l) SEM images of surface-bound CD4 T-lymphocytes on four different sizes of QNHs (a-c 140 nm, d-f 200 nm, g-i 270 nm, and j-l 550 nm in diameter) with top, tilt and enlarged views. All of surface-bound T-lymphocytes were highlighted in blue for easy differentiation.

observation was performed. For SEM observation of the captured cells on QNHA substrate, several cell-fixing processes are required as follows. The T-cells were first fixed with 4% GA in the refrigerator for 2 hr, followed by a post-fix process using 1% osmium tetroxide for 2 hr. The captured T-lymphocytes were then dehydrated through a series of ethanol concentrations (25, 50, 75, 95, and 100%) and slowly dried at vacuum-connected desiccators for 24 hr [7, 9]. Once the samples were dry in the desiccators, the surface-bound T-lymphocytes were sputter-coated with platinum before performing the FE-SEM measurement.

3. RESULTS AND DISCUSSIONS

Figs. 2a-d show scanning electron microscope (SEM) images, showing the tilt-views of QNHAs prepared with four different sizes of PS nanoparticles. The diameters of

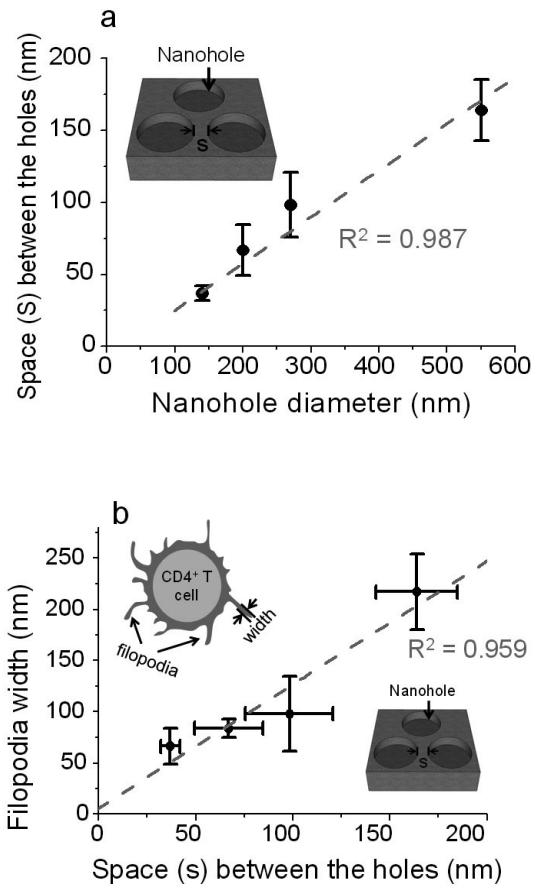

Fig. 4. (a) The space between the nanoholes as a function of the diameters of prepared QNHA (140, 200, 270, and 550 nm), indicating strong linear relationship between them. (b) The distribution of filopodia width of surface-bound T-cells on the four different sizes of QNHAs.

QNHA using four PS NPs (200, 300, 430, and 750 nm in diameter) were to be 140, 200, 270, and 550 nm, respectively as determined by SEM. As shown in Figs. 2a-d, all of the QNHA were well defined on the quartz substrates. To further exhibit a flexibility of the size and structures of QNHA, the further wet-chemical etching was performed for 10 up to 100 s using buffered oxide etchant (BOE) solution. As shown in Figs 1e-g, these results suggest that the QNHA structures can be easily fabricated in the different size formation using both RIE dry and further wet-chemical etching process. We also believe these different kinds of QNHA structures provide more information platform that provides valuable information about adhesion and migration of the captured cells to nanostructured substrates. Figs. 3a-l show FE-SEM images, showing top, tilt and enlarged views of $CD4^+$ T lymphocytes, bound on the surface of STR-functionalized QNHA with four different size of diameters (140, 200, 270, and 550 nm). The detailed morphologies of the captured T-cells on STR-QNHA substrates were examined by quantitative FE-SEM analysis (Figs. 3a-l). These results exhibit that the captured T-cells were well bound on the surface with different morphologies of filopodia or lamellipodia. Interestingly, these images indicate that the morphology of microvilli including filopodia or lamellipodia of the capture T-cells is highly correlated with the size of QNHA in diameter from 140 to 550 nm or space between the nanoholes of QNHA. As shown in Fig. 4a, we found that the higher QNHA substrates in diameter produces the higher space between the each hole of QNHA with almost unit of R^2 value (R^2=0.987, n=10, Fig. 4a). To verify the results, more than 6-10 cells were selected and analyzed on the same QNHA substrates. Fig. 4b exhibits that the extended filopodia of the captured $CD4^+$ T-cells were observed to increase in width by increasing the diameter of QNHA from 140 to 550 nm, resulting in a good linear response between the width of T-cells and diameter of QNHA (R^2=0.959, n=10). These results suggest that the microvilli (filopodia or lamellipodia) of $CD4^+$ T-cells closely react with the QNHA substrates via high-affinity STR-biotin conjugation [7] as we proved previously and extend filopodia of different lengths or widths depending on the diameter of the QNHAs as an alive sensor system to detect the size of the structures underneath of the cells using microvilli (Figs. 3a-l). This strong linear response in filopodia extending from the T-cells bound on the solid-state surfaces with the nanohole

size (e.g. diameter) of the surface could be explained by a contact guidance phenomenon, which is normally used to explain the behavior of fibroblast filopodia on nanostructured substrates with a long incubation [15-17]. According to contact guidance phenomenon, the T-cells extend filopodia to recognize and sense the surface features of nanotopography substrates when they are bound on the surface at the early state of the adhesion, and then form themselves on the substrates with a similar size of the nanostructure underneath the cells. Similar results were reported by Dalby et al.[18, 19]. They observed that filopodia increased in thickness with an increase in the size of the island topography from 13 to 95 nm, which is in good agreement with our results in Fig. 4b even they used epithelial cell-line instead of T-cells.

4. CONCLUSIONS

In conclusion, we first utilized surface-bound live T-cells via STR-biotin conjugation method as a biosensor to sense the size of the nanostructures (in our case, nanoholes). We observed that the higher QNHA substrates in diameter produce the higher space between the each hole of QNHA. Furthermore, the extended filopodia of the captured $CD4^+$ T-cells were observed to increase in width by increasing the diameter of QHNA from 140 to 550 nm, resulting in a good linear response between the width of T-cells and diameter of QNHA. This strong linear response in filopodia extending from the T-cells bound on the solid-state surfaces with the nanohole size (e.g. diameter) of the surface could be explained by a contact guidance phenomenon.

ACKNOWLEDGMENT

This study was supported by the Priority Research Centers Program and by the Basic Science Research Program through the National Research Foundation of Korea (NRF) funded by the Ministry of Education, Science and Technology (2011-0027956, PI: S.K.L.). This work was also supported by a grant from the Global Excellent Technology Innovation R&D Program, funded by the Ministry of Knowledge Economy, Republic of Korea (10038702-2010-01).

REFERENCES

[1] J. M. Lorcy, F. Massuyeau, P. Moreau *et al.,* "Coaxial nickel/poly(p-phenylene vinylene) nanowires as luminescent building blocks manipulated magnetically", *Nanotechnology,* Vol. 20, No. 40, p. 405601, 2009.

[2] S. Schafer, Z. Wang, R. Zierold *et al.,* "Laser-induced charge separation in CdSe nanowires", *Nano Lett.,* Vol. 11, No. 7, pp. 2672-2677, 2011.

[3] P. D. Yang, R. X. Yan, and M. Fardy, "Semiconductor nanowire: What's next?", *Nano Lett.,* Vol. 10, No. 5, pp. 1529-1536, 2010.

[4] K. S. Brammer, C. Choi, C. J. Frandsen *et al*., "Hydrophobic nanopillars initiate mesenchymal stem cell aggregation and osteo-differentiation", *Acta Biomater.,* Vol. 7, No. *2,* pp. 683-690, 2011.

[5] W. Kim, J. K. Ng, M. E. Kunitake *et al.,* "Interfacing silicon nanowires with mammalian cells", *J. Am. Chem. Soc.,* Vol. 129, No. 23, pp. 7228-7229, 2007.

[6] Jianping Fu, Yang-Kao Wang, Michael T Yang *et al.,* "Mechanical regulation of cell function with geometrically modulated elastomeric substrates", *Nat. Methods,* Vol. 7, No. 9, p. 799, 2010.

[7] S. T. Kim, D. J. Kim, T. J. Kim *et al.,* "Novel streptavidin-functionalized silicon nanowire arrays for CD4(+) T lymphocyte separation", *Nano Lett.,* Vol. 10, No. 8, pp. 2877-2883, 2010.

[8] S. K. Lee, G. S. Kim, Y. Wu *et al.,* "Nanowire substrate-based laser scanning cytometry for quantitation of circulating tumor cells", *Nano Lett.,* Vol. 12, No. 6, pp. 2697-2704, 2012.

[9] D. J. Kim, J. K. Seol, Y. Wu *et al.*, "A quartz nanopillar hemocytometer for high-yield separation and counting of CD4(+) T lymphocytes", *Nanoscale,* Vol. 4, No. 7, pp. 2500-2507, 2012.

[10] Anselme K, Davidson P, Popa A M *et al.,* "The interaction of cell and bacteria with surfaces structured at the nanometre scale", *Acta Biomater.,* Vol. 6, p. 3824, 2010.

[11] Xuanhong Cheng, Amit Gupta, Chihchen Chen *et al.,* "Enhancing the performance of a point-of-care $CD4^+$ T-cell counting microchip through monocyte depletion for HIV/AIDS diagnosis", *Lab Chip,* Vol. 9, No. 10, pp. 1357-1364, 2009.

[12] Park N K et al., "The correlation of serum HER-2/neu and CA 15-3 in patients with metastatic breast cancer", *J. Breast Cancer,* Vol. 11, pp. 18-24, 2008.

[13] Yair Fisher, Anna Nemirovsky, Rona Baron *et al.,* "The correlation of serum HER-2/neu and CA 15-3 in patients with plaques enhance plaque clearance in a mouse model of Alzheimer's disease", *PloS one,* Vol. 5, No. 5, p. e10830, 2010.

[14] D. J. Kim, J. K. Seol, Geehee Lee *et al.,* "Cell adhesion and migration on nanopatterned substrates and their effects on cell-capture yield", *Nanotechnology,* Vol. 23, p. 395102, 2012.

[15] C. J. Bettinger, R. Langer, and J. T. Borenstein, "Engineering substrate topography at the micro- and nanoscale to control cell function", *Angew. Chem. Int. Edit.,* Vol. 48, No. 30, pp. 5406-5415, 2009.

[16] M. J. Dalby, "Topographically induced direct cell mechanotransduction", *Med. Eng. Phy.,* Vol. 27, No. 9, pp. 730-742, 2005.

[17] M. J. Dalby, N. Gadegaard, M. O. Riehle *et al.,* "Investigating filopodia sensing using arrays of defined nano-pits down to 35 nm diameter in size", *Int. J. Biochem. Cell B.,* Vol. 36, No. 10, pp. 2005-2015, 2004.

[18] A. Hart, N. Gadegaard, C. D. W. Wilkinson *et al.*, "Osteoprogenitor response to low-adhesion nanotopographies originally fabricated by electron beam lithography", *J. Mater. Sci.-Mater. M.,* Vol. 18, No. 6, pp. 1211-1218, 2007.

[19] M. J. Dalby, M. O. Riehle, H. J. H. Johnstone *et al.,* "Polymer-demixed nanotopography: Control of fibroblast spreading and proliferation", *Tissue Eng.,* Vol. 8, No. 6, pp. 1099-1108, 2002.